Local-density approximation study of semiconductor/metal adsorption characteristics: Ge/Ag(100)

S. Sawaya, J. Goniakowski, and G. Tréglia
Centre de Recherche sur les Mécanismes de la Croissance Cristalline, CNRS, Campus de Luminy, Case 913, 13288 Marseille Cedex 9, France
(Received 15 December 1998)

Using the *ab initio* full-potential linear muffin-tin orbital approach, we have studied the characteristics of Ge adsorption on the Ag(100) surface. We have determined the preferential adsorption site and analyzed the adsorption-induced modifications of electronic structure of both the substrate and the adsorbate. By considering three model epitaxial deposits 1.0, 0.50, and 0.25 Ge ML we have accessed the characteristics of the evolution of the adatom-surface bonding as a function of the amount of deposited germanium. We report a very clear site and coverage dependence of the measurable physical parameters, which can be directly used for analysis of experimental data. [S0163-1829(99)05623-4]

I. INTRODUCTION

For the last decade, major efforts have been focused on the understanding of the properties of metal-semiconductor interfaces. This is mainly due to their direct technological applications but also to the wide range of very fundamental questions that arise from the studies on these systems.[1] Basic goals of the research include a description of the metal-semiconductor interface chemistry on an atomic level, and a characterization of the interface electronic structure. Most of the work carried out until now has been performed by depositing metal films on semiconductor surfaces (M/S),[2–8] reflecting the historical evolution of metal/semiconductor devices. It is only very recently that a growing interest on semiconductors deposited on metal surfaces (S/M) is to be noticed and this is why much fewer studies concerning the reverse situation exist.[9–11] Since, especially on the early growth stages, the properties of the S/M and M/S systems are not necessarily symmetrical, we believe that such studies are important for a better understanding of the properties of the metal-semiconductor interface. A question of particular interest is the evolution of respective metallic and semiconducting character under the mutual influence of the two components as a function of the growth mode and deposit coverage. In this context, on a more applied level, the properties of the (potentially) self-assembling semiconductor nanoparticles on a metal support are likely to rise a significant industrial interest.

During the deposition, the electronic and atomic structures of both the substrate and the deposit are affected by their mutual interaction. For the former, this consists mainly in changes of the local density of states (LDOS) at the Fermi level. For the latter, it leads to different adsorption characteristics depending on the respective weights of the metallic (tendency to maximize the coordination of the adsorbate) or semiconductor (orientational bonding due to sp^3 orbitals) characters. In fact, very recent experiments of Ge deposition on the Ag (100) surface show that the early atomic structure of the deposit is relatively complex and does not directly reflect neither semiconductor nor metal-like adsorption tendencies.[12]

In order to better understand the fundamental process responsible for the physical properties of the semiconducting deposit and to furnish the experimentalists with a guideline to the analysis of their findings, we have undertaken an *ab initio* density functional study of Ge deposit on the Ag(100) surface. On the basis of the numerical results, we have analyzed the microscopic effects in terms of simple chemical concepts based on the atomic orbitals involved in the Ge-surface bonding. We have focused our attention on the comparison between the calculated electronic structures of three alternative surface adsorption sites, and on discussion of their dependence on Ge coverage. In the present study we have considered only model, epitaxial structures of the deposit, neglecting all reconstruction effects. This strategy, although not giving the possibility of a direct comparison with a particular set of experimental results, has the advantage of giving a relatively clear physical picture of microscopic mechanisms which determine the properties of the deposit and constitute a well defined basis for the future studies (by effective approaches). Additionally, calculated evolution of experimentally accessible signatures of modifications of the electronic band structure can be used directly for a qualitative analysis of experimental spectra.

The paper is organized as follows: in Sec. II we briefly outline the numerical approach used for the present study. In Sec. III we present the results concerning the adsorption of an isolated Ge atom and the coverage dependence of the adsorbate characteristics. Section IV contains the results on the core electrons binding energy and on the surface charge density distribution. Concluding remarks are presented in Sec. V.

II. COMPUTATIONAL DETAILS

The theoretical framework chosen for the present study is based on the density functional theory[13] (DFT) within the local density approximation (LDA).[14] The Ceperley-Alder form of the exchange-correlation energy functional was used.[15] The one-particle Kohn-Sham equations were solved self-consistently using the all-electron full-potential linear muffin-tin orbitals (FP-LMTO) method,[16,17] for which no ap-

proximation on the shape of the charge density and one-particle potential makes it adequate for low symmetry systems such as surfaces and interfaces.[18,19] Within the FP-LMTO method the space is divided into nonoverlapping spheres centered on atomic sites. The basis set consists of atom-centered Hankel envelope functions which are augmented inside the atomic spheres by means of numerical solutions of the scalar-relativistic Dirac equation. Due to the nonvanishing interstitial region, it is enough to use the minimal basis set: we have used three *s*, three *p*, and three *d* partials waves with kinetic energies of -0.7, -1.0, and -2.3 Ry, thus, 27 functions per sphere. The ''two-panel'' technique was used to include the $3p$ $3d$ electrons of germanium and the $4p$ semicore electrons of silver as full band states. Valence states are Ge($4s$ $4p$ $4d$) and Ag($5s$ $5p$ $4d$). In order to eliminate any possible errors due to changes of the basis set, atomic muffin-tin radii were fixed to 2.35 a.u. for Ag and 2.00 a.u. for Ge for all the calculations presented in this paper. We have verified that using a different set of muffin-tin radii leads to only small differences in the adsorption energies and in the equilibrium geometries. In any case it does not modify the calculated tendencies.

To obtain an accurate representation of the exponentially decaying density outside the surface, in slab calculations it is often necessary to cover the surface with one or several layers of empty spheres. In the present calculations the adsorbed Ge atoms were covered with a single layer of empty spheres. For 0.50 and 0.25 ML coverage, the missing Ge adatoms were also replaced by the empty spheres. The empty-sphere angular-momentum cutoff for charge density and for the augmentation of the wave function was fixed to 6 and 4, respectively.

The **k**-point summation was done on a uniform mesh in the irreducible wedge of the Brillouin zone and converged to within 10 meV/atom for 121 **k** points in the Brillouin zone. For a better numerical stability, a Gaussian broadening of $\sigma=20$ mRy was used in all the calculations.

We have verified that the bulk equilibrium properties of both Ag and Ge are reproduced correctly. In particular for Ag, the lattice parameter $a_0^{th}=4.00$ Å, the bulk modulus $B^{th}=140$ GPa, and the cohesive energy $E_{coh}^{th}=3.69$ eV, compare fairly well with the experimental low-temperature values ($a_0^{\exp}=4.09$ Å, $B^{\exp}=101$ GPa, and $E_{coh}^{\exp}=2.95$ eV).[20] For Ge, the calculated bulk lattice constant $a_0^{th}=5.57$ Å, the bulk modulus $B^{th}=90$ GPa and the cohesive energy $E_{coh}^{th}=4.85$ eV, present a similar overall agreement with the low-temperature experimental data: $a_0^{\exp}=5.66$ Å, $B^{\exp}=77$ GPa, and $E_{coh}^{\exp}=3.87$ eV.[20] Systematic underestimation of the lattice parameter a_0 and overestimation of the bulk modulus B and cohesive energy E_{coh} are typical for the LDA approximation.

Both clean and Ge-covered Ag(100) surfaces were modeled by five-layer-thick slabs, separated by seven layers of vacuum (about 28 Å). The lattice constant a_0^{th} determined for the bulk silver and the $(\sqrt{2}\times\sqrt{2})R45°$ surface cell were systematically used in all slab calculations. We have verified that in this framework the surface energy converges within 10 meV. Deposition of four, two and one Ge adatom per surface cell, corresponds respectively to 1.0, 0.50, and 0.25 ML coverage.

TABLE I. Evolution of the number of neighbors of both Ge and surface Ag as a function of adsorption site and Ge coverage: $Z_{tot}^{A}(Z_{AA},Z_{AB})$ where A, B denote Ge or Ag, and $Z_{tot}^{A}=Z_{AA}+Z_{AB}$.

	adsorption site \ θ	0.25	0.5	1.0	bulk
Ge	on-top	1 (0,1)	3 (2,1)	5 (4,1)	4 (4,0)
	bridge	2 (0,2)	4 (2,2)	6 (4,2)	
	hollow	4 (0,4)	6 (2,4)	8 (4,4)	
Ag	on-top	9 (8,1)	9 (8,1)	9 (8,1)	12 (12,0)
	bridge	9 (8,1)	10 (8,2)	10 (8,2)	
	hollow	9 (8,1)	10 (8,2)	12 (8,4)	

In all calculations the positions of substrate atoms were not optimized. On one hand, for a clean metal surface, it is known that the modification of the surface energy due to the surface relaxation is small and that the interatomic distances change by only a few percent.[18] On the other hand, in order to estimate the contribution to the adsorption energy due to the substrate relaxation, we have tested the case of adsorption of an isolated Ge atom on top of a surface Ag one. In this case, for which modification of the substrate characteristics is the most pronounced, we have optimized simultaneously both the vertical positions of the adsorbate and of the surface atoms. This relaxation of the substrate atom induced only a 2% increase of the adsorption energy and 1.5% increase of the Ge-Ag distance.

III. RESULTS

In the following we will present the results concerning the adsorption energetics and the characteristics of the electronic band structure for Ge deposited on the Ag (100) surface. We will start by considering the adsorption characteristics of an isolated Ge adatom deposited in the three inequivalent surface adsorption sites. Further on, we will present the evolution of the adsorption characteristics as a function of increasing coverage of deposited germanium. Schematically, the first part will give us information on the influence of the number of Ge-Ag bonds on both substrate and adsorbate electronic structure. The second part will allow to analyze the respective contributions of the Ge-Ge and Ge-Ag bonds to the overall adsorption characteristics (see Table I).

A. Adsorption of an isolated Ge atom

In our calculations, adsorption of 0.25 ML of Ge corresponds to the deposition of a square lattice of germanium adatoms, separated by 5.65 Å. Since in this configuration the direct interaction between two Ge atoms is negligible, we will consider it as a good approximation for adsorption of isolated Ge atoms.

1. Preferential adsorption site

In order to determine the preferential adsorption site for adsorption of an isolated Ge atom, we have evaluated the adsorption energy for three inequivalent surface adsorption

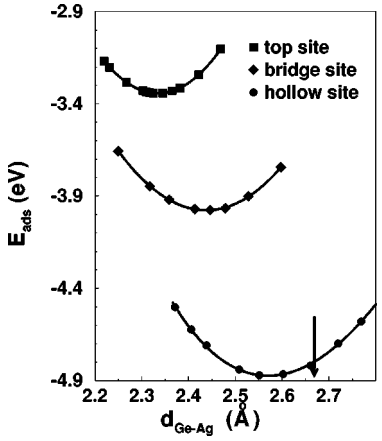

FIG. 1. Adsorption energy, E_{ads} (eV), as a function of the Ge-Ag nearest-neighbor distance d_{Ge-Ag} (Å) calculated for adsorption of a single Ge adatom in the hollow, bridge, and on-top Ag(100) surface adsorption sites. The arrow indicates the sum of pure elements atomic radii.

geometries: on-top, on-bridge, and in the hollow surface site (the center of a square formed by four surface atoms). For the (100) surface, germanium atoms adsorbed in the three considered sites have respectively one, two, and four nearest neighbors (see Table I). In Fig. 1 we display the corresponding calculated dependence of the adsorption energy on the distance between the deposited germanium atom and its surface silver first neighbors. Adsorption energy is given with respect to a free germanium atom:

$$E_{ads}=\tfrac{1}{2}(E^{Ge/Ag(100)}-E^{Ag(100)}-2E^{Ge}_{atom}),$$

$E^{Ge/Ag(100)}$, $E^{Ag(100)}$, and E^{Ge}_{atom} being the total energies of the adsorbate-covered slab, of the clean slab, and of the free Ge atom respectively. The factor 1/2 accounts for the fact that the Ge adatoms are deposited symmetrically on both sides of the slab. It is worth noting that since adsorption geometries are not equivalent, the Ag-Ge first neighbors distance is not directly representative for the vertical Ge-surface distance. In fact, the greatest the coordination of Ge, the longer the Ge-Ag bond, but the lowest the Ge elevation above the surface.

The hollow site appears to be energetically the most favorable for adsorption, the on-bridge and on-top sites having their energy minima respectively 0.9 and 1.5 eV higher. It is worth noticing that this geometry allows both Ge and Ag atoms to keep their respective atomic volumes ($d_{Ge-Ag} \simeq r^{Ge}_s + r^{Ag}_s$), thus avoiding any size-mismatch stress. This preference for the hollow site can be interpreted differently depending on that it is viewed as the best way for Ge either to maximize its number of neighbors (metalliclike character) or to recover the same number of neighbors (four) as in its own bulk (covalentlike character). However, one has to keep in mind that the orientational sp^3 bonds occuring in the latter case (Ge in the center of a tetrahedron) have nothing to do with the present situation (Ge on top of a pyramid), so that the present result is rather the signature of a preferential metallic character of adsorption. The tendency to maximize the number of neighbors (as for M/M adsorption[21,22]) imposed by the metallic character of the substrate, instead of saturating dangling bonds in a preferential orientation manner, seems to be a rather general rule played by adsorbates of different natures. Jentz *et al.*[23] by low-energy electron diffraction (LEED) on sulfur and carbon overlayers on Mo(100), found the adsorbed adatoms at or near the fourfold coordinated sites. Similar LEED experiments on H chemisorbed on Pd(111) by Eberhardt *et al.*[24] suggested adsorption of H at the highest coordinated threefold surface site.

A very well pronounced tendency can be also seen in the evolution of the Ge-Ag bond length, which is the shortest (2.33 Å) for the on-top adsorption site and becomes progressively longer for the bridge and hollow sites (2.44 and 2.56 Å, respectively) tending towards the sum of atomic radii in the last case. Here also the increase of the bond length with increasing number of bonds created in the adsorption process is typical for a metal adatom adsorption on a transition metal surface. This tendency can be explained on the basis of a simple tight-binding model,[25] and is systematically reported by recent *ab initio* calculations (see, e.g., Ref. 26). It is also worth noting that the Ge-Ag bond length deduced from the LEED I-V experiments by Huang *et al.*[27] on Ag deposition on the Ge(111) surface (2.52 ± 0.09 Å) is consistent with our results, which suggests that it is an intrinsic characteristics of the M-S interactions and depends little on the particular M/S or S/M growth mode.

Finally, similar results issued from semiempirical calculations have been recently reported for Ga deposition on Ag (100).[28] The authors find the four-fold hollow site preferred for adsorption by about 1 eV with respect to the bridge and on-top ones. The reported Ga-Ag bond lengths, and their evolution as a function of the adsorption site correspond also well to the present findings. Although this correlation could appear as natural judging by the relative positions of Ga and Ge in the periodic table, it is however important to underline that their respective bulk and surface properties are sensibly different.

2. Adsorption versus substitution

By analogy with situation often encountered for M/M deposit, and to complete the study we have also considered the case in which the Ge adatom is substituted in place of one surface Ag atom, rather than adsorbed on the surface. In this case, the formation energy can be calculated as

$$E_{sub}=\tfrac{1}{2}(E^{Ge/Ag(100)}-E^{Ag(100)}-2E^{Ge}_{atom}+2E^{Ag}_{bulk}),$$

$E^{Ge/Ag(100)}$, $E^{Ag(100)}$, E^{Ge}_{atom}, and E^{Ag}_{bulk} being the total energies of the Ag slab including the Ge substituted atoms, of the clean Ag slab, of the free Ge atom, and of the Ag atom in its own bulk, respectively. The microscopic process corresponds thus to replacement of a surface Ag atom by a free Ge one, the Ag atom being reintegrated into the bulk or equivalently moved to a kink. We have verified that the modification of the substitution energy due to the relaxation of Ge is small (about 0.02 eV/atom) and that the interatomic distances between Ge and Ag change by less than 2%.

We find that energetically this final configuration is by 0.33 eV more stable than the adsorption in the hollow surface site, discussed in the previous paragraph. However, one needs to keep in mind that the reference energetics for adsorption and substitution are not fully equivalent, so that any direct comparison of formation energies may be misleading.

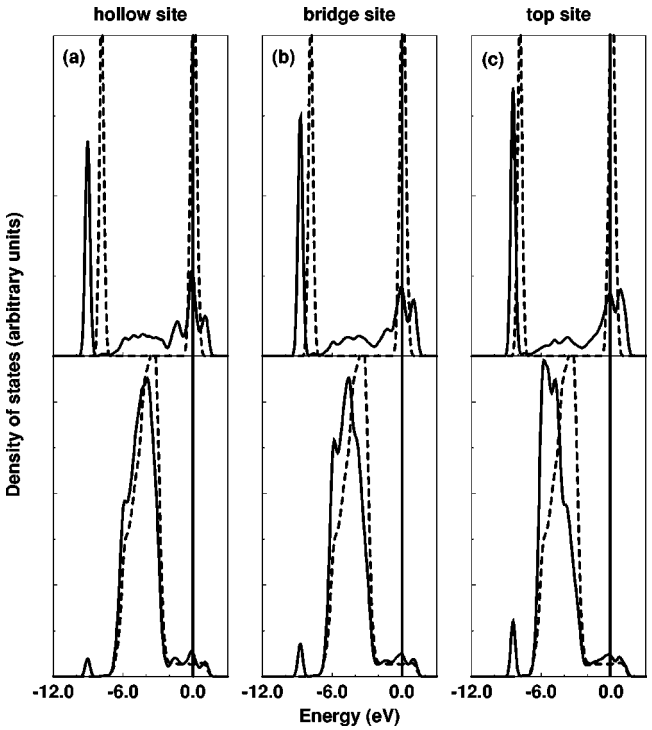

FIG. 2. Local DOS calculated for a single Ge adatom deposited in the hollow (a), bridge (b), and on-top (c) Ag(100) surface sites. Both Ge projected (upper panel) and surface Ag projected (lower panel) DOS are plotted. Dashed lines represent the LDOS for separated systems.

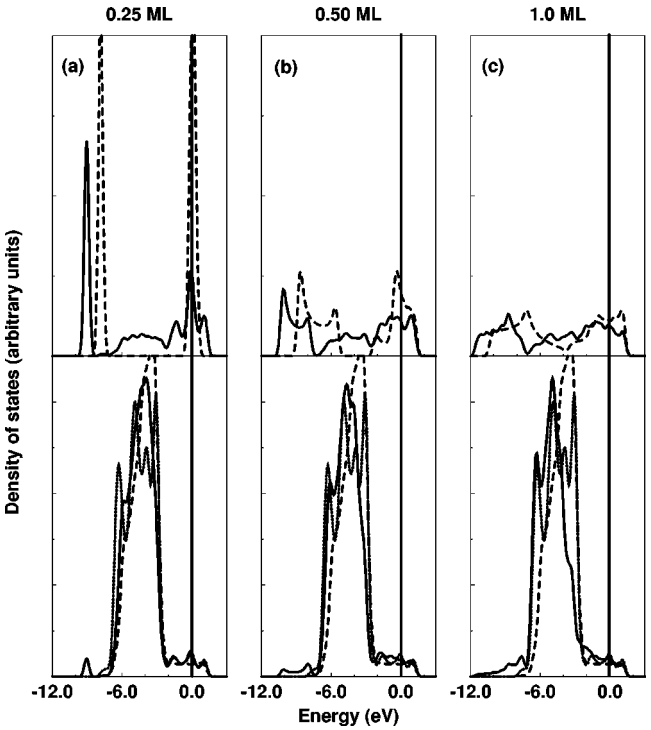

FIG. 3. Local DOS calculated for the 0.25 ML (a), 0.50 ML (b), and 1.0 ML (c) Ge deposit in the hollow Ag (100) surface sites. Both Ge projected (upper panel) and surface Ag projected (lower panel) DOS are plotted. The dashed lines represent the LDOS for separated systems, and the dotted lines the Ag bulk one.

Additionally, since the substitution energy is to a large extent dominated by the E_{bulk}^{Ag} term, the latter being overestimated by the LDA approach, this could possibly induce further errors.

Finally, as it has been already pointed out before, a thermal activation (in the form of creation of surface vacancies) is necessary for activation of the substitutional adsorption mode. At temperatures sufficient to activate surface diffusion of Ge but not high enough to create surface vacancies, the adsorption will take place principally at adatom positions.

3. Densities of states

In order to relate the site dependence of adsorption characteristics to the modifications of the electronic structure we present in Fig. 2 the local (projected on the atomic spheres) densities of states (LDOS) obtained for the three different adsorption geometries considered. Since we have verified that the adsorption-induced modifications of the substrate DOS are limited principally to the surface layer, in the figure we show the projection on the surface adsorption site only. The dashed lines represent the LDOS of the separated systems: of an isolated Ge atom and of an Ag atom of the surface layer on the clean (100) surface. For the different adsorption geometries, the energy scales were aligned as to superpose the DOS projected on the Ag atom in the center of the slab (not shown in this figure, but see Fig. 3). The DOS of free Ge atoms were shifted as to align the corresponding Fermi levels. The LDOS of a clean Ag (100) surface is dominated by the 4*d* band centered at about 4 eV below the Fermi level, thus about 0.4 eV higher than the bulk 4*d* band (see Fig. 3). The 5*s* and 5*p* bands hybridize with the 4*d* one and give the dominant contribution around the Fermi level. For all three adsorption geometries, adsorption of an isolated Ge atom induces two main modifications of the substrate DOS. On the one hand, the center of gravity of the 4*d* band is shifted towards lower energies. With respect to the clean surface, we find shifts of -0.28 eV, -0.45 eV, and -0.64 eV for adsorption in the hollow, the bridge, and the on-top sites, respectively. This evolution reflects the increase of the Ge-Ag bond strength (seen already in the shortening of the Ge-Ag bond length) when passing from a more to a less coordinated adsorption site. On the other hand, due to the interaction with the *sp*-shell of Ge, an additional peak appears below the 4*d* band. Both its position and size change as a function of the adsorption geometry. In particular, higher coordination of the adsorption site corresponds to its larger downward shift and smaller intensity. Again, this is a clear signature of weakening of Ge-Ag bonds with their increasing number.

Let us now analyze the evolution of the LDOS of germanium. A free atom is characterized by the 4*s* and 4*p* Dirac-like peaks (in the figure, systematically a Gaussian broadening of 20 mRy was used), separated by about 7.7 eV. The Fermi level intersects the latter one, giving the atomic paramagnetic ground state $4s^2 4p^2$. The adsorption-induced modifications of the germanium LDOS are twofold. On the one hand we find that both germanium *s* and *p* states hybridize with the substrate *d* band, giving for all considered adsorption geometries a clear contribution in the *d* band energy region. On the other hand, both *s* and *p* peaks are modified upon the adsorption. The former is significantly damped and

shifted downwards on the energy scale. This downward shift increases with the increasing coordination of the adsorption site, we find 0.6, 0.9, and 1.2 eV for the three sites, respectively. Germanium p states clearly hybridize with the Ag band, and a non-negligible part is pushed above the Fermi level. This tendencies are compatible with existence of one stronger Ag-Ge bond (on-top site), evolving into four weaker ones (hollow site).

Modifications of the electronic structure of a similar character were already reported for Ge deposited on the Cu (111) surface. When studied by the angle-resolved direct and inverse photoemission,[29] a 0.5 eV downward shift of the Cu d band with respect to the clean surface spectrum was observed. Also Weaver *et al.*[30] have reported a coupled synchrotron radiation photoemission and ASW energy-band calculation study of metal silicides. They found a lowering of metal-derived $3d$ states that hybridize with Si-derived $3p$ states.

B. Dependence on the Ge coverage

In order to get information on the dependence of adsorption characteristics on the germanium coverage, we have considered three model germanium deposits corresponding to 0.25, 0.50, and 1.0 ML coverage in the three inequivalent adsorption geometries (see Table I). At 0.25 ML coverage the configuration corresponds to the nearly isolated atom adsorption, which has been discussed in the preceding section. In this adsorption geometry Ge adatoms do not have Ge first neighbors. At 0.50 ML the deposit consists of parallel rows spaced by 5.65 Å formed by germanium adatoms. Within the row, each Ge atom has two Ge neighbors spaced by 2.83 Å (compared to 2.42 Å in the bulk germanium). Finally, at 1.0 ML the germanium adatoms occupy a square lattice of Ag lattice parameter. Each Ge atom has thus four Ge neighbors at 2.83 Å.

It is worth underlining that although the full geometry optimization of the deposit does not enter in the scope of this paper, the considered germanium configurations cover the range of germanium coordination numbers characteristic for the atomic environment in small germanium clusters, on the Ge (111) surface, as well as in the bulk germanium (see Table I). Let us recall, however, that the corresponding bond lengths are significantly larger than the bulk ones. The considered configurations can be thus considered as representative for prototypes of systems with a more complex atomic structure and can furnish the information useful for constructing effective potentials necessary for a full-scale dynamical study of Ge deposit on the Ag (100) surface.

1. Adsorption energetics

The adsorption energy is defined, as previously, with respect to isolated germanium atoms as a reference:

$$E_{ads}=\frac{1}{2N}(E^{Ge/Ag(100)}-E^{Ag(100)}-2NE^{Ge}_{atom}),$$

where N is now the number of Ge atoms per surface unit cell. In this way one obtains the gain in energy due to new bonds (both Ge-Ge and Ge-Ag) created within the adsorption process together with the contribution due to the adsorption-induced change of the Ag-Ag bonding (decohesion) in the substrate.

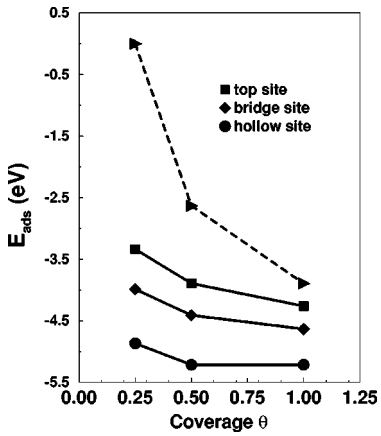

FIG. 4. Adsorption energy E_{ads} (eV) as a function of the Ge coverage, calculated for adsorption in the hollow, bridge, and on-top Ag(100) surface sites. Dashed line represents the cohesive energy of the floating (strained) Ge deposit.

In Fig. 4 we have compiled the numerical results concerning the energetics of adsorption of germanium deposits as a function of coverage in three inequivalent adsorption geometries. The general tendency of E_{ads} is an enhancement of the adsorption energy when the coverage increases, which is consistent with the fact that more Ge-Ge bonds are created upon adsorption of Ge atoms. However, this change of adsorption energy is significantly site dependent. It is smaller for more coordinated adsorption sites, indicating a saturation of adsorption energy with increasing number of neighbors. We find a change of about -0.92, -0.64, and -0.35 eV when passing from 0.25 to 1.0 ML coverage for, respectively, on-top, bridge, and hollow adsorption sites. At the same time, in all considered cases, this energy gain is much smaller than the cohesive energy of the floating, unrelaxed deposit (see dashed line in Fig. 4). It is thus clear that the overall adsorption energetics cannot in any case be approximated by a simple sum of Ag-Ge and Ge-Ge interactions only, and that both substrate Ag-Ag bonds and Ge-Ge bonds in the deposit are modified by the adsorption. In particular, it is worth noticing that this correlated evolution of the bonding character makes that for the preferential adsorption site (hollow site) the adsorption characteristics are practically coverage-independent. This is partially due to the fact that the considered deposit is epitaxial (the Ge-Ge bond lengths were elongated by 17%, as to match the Ag-Ag distances), but we have verified that in all cases, the energy necessary to elongate the Ge-Ge bonds is small compared to the cohesive energy of the deposit.

The trends of evolution of the bond lengths across the series of configurations are unambiguous (Fig. 5). In all cases we observe a dilation of Ge-Ag distances, when the coverage increases. This coverage-induced effect remains however relatively small—we find an increase of 6%, 6%, and 3% for hollow, bridge, and on-top sites respectively. In all cases the maximal variation does not exceed 6%, while the variation of Ge-Ag distance as a function of adsorption site is of the order of 11%.

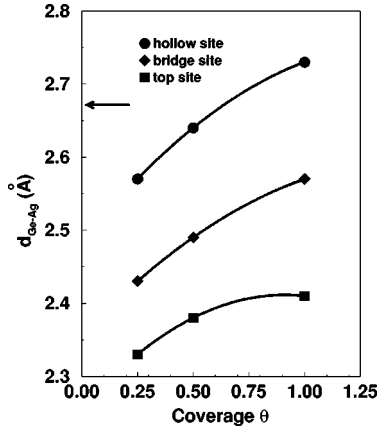

FIG. 5. Ge-Ag nearest-neighbor distance d_{Ge-Ag} (Å), as a function of the Ge coverage, calculated for adsorption in the hollow, bridge, and on-top Ag(100) surface sites.

2. Densities of states

We will now focus on the modification of the interface electronic structure related to changes of the Ge coverage. In order to simplify the presentation, in the following we only show the LDOS obtained for the preferential adsorption site. Figure 3 depicts the LDOS obtained for the three different coverage rates. As before, full and dashed lines correspond, respectively, to Ge/Ag(100) and to separated systems [Ag of a clean (100) surface and a floating unsupported germanium deposit]. The energy scales were aligned as to superpose the DOS projected on the Ag atom in the center of the slab (see the dotted line in Fig. 3). The DOS of free Ge deposits were shifted as to align the corresponding Fermi levels.

For the three coverage rates, the adsorption-induced modifications of the substrate DOS have principally a twofold character. On the one hand, the center of gravity of the Ag $4d$ band is shifted towards lower energies, i.e, towards bulk Ag. With respect to the clean surface, we find a shift of -0.28 eV, -0.52 eV, and -0.82 eV for adsorption of 0.25, 0.50, and 1.0 ML of germanium, respectively. As can be seen by comparison with Ag bulk LDOS which is shifted by ~ -0.4 eV with respect to surface, this is consistent with more and more bulklike character of surface Ag atoms (from the point of view of their coordination). In fact, the surface atoms even go beyond bulk character (we will come back on this point later). On the other hand, due to the interaction with the sp band of Ge, an additional structure appears below the $4d$ band. Its width and the degree of hybridization with the $4d$ one increase with increasing coverage, following the evolution of the LDOS of the unsupported Ge deposit. Similar tendency was already reported for Si deposited on the amorphous Au for which the photoemission study by Franciosi *et al.*[31] showed an increasing shift of the Au d band to higher binding energies which can be correlated to the increasing coverage rate of the Si deposit.

The adsorption-induced modifications of the germanium LDOS consist principally in an overall broadening of the deposit valence band. As it can be clearly seen for the isolated atom adsorption, the origin of this broadening is twofold. On the one hand germanium s states are shifted downwards, on the other hand the p states hybridize with the substrate band. With increasing coverage, the hybridization between the s and p states of germanium increases, and the separation of the two effects becomes less justified.

IV. MEASURABLE CHARACTERISTICS OF THE ELECTRONIC AND ATOMIC STRUCTURE OF THE DEPOSIT

In the present section we discuss the principal experimentally accessible signatures of the electronic structure of the Ge/Ag(100) system, focusing on their relation with the atomic structure. We start by an analysis of the adsorption induced core level shifts on the Ag surface atoms and of their dependence on both adsorption site and Ge coverage. We finish by a simple simulation of STM images of a Ge deposit on the Ag(100) surface, discussing them in context of similar results existing for the Ga/Ag(100) system.

A. Binding energy of core electrons

It is well known that the core-level binding energies depend upon the atomic and chemical environment, and can thus contain the information on the local structure. For example, since the local atomic environment of atoms in the bulk of a crystal differs from that at the surface, surface atoms generally exhibit different core-level energies than atoms in the bulk. Similarly, deposition of atoms on the surface can alter the local atomic environment of some surface sites. In general, this modification depends not only on the site on which the adatoms adsorbs, but it also varies with the adsorbate coverage.[32] At the same time, both the type of adsorption site and the adsorbate coverage do influence the binding energy of the adsorbate core electrons. Thus, the high-resolution core-level photoemission experiments on both the substrate and adsorbate core levels can often provide vital clues for the deduction of the adsorbate-substrate interface structure.

A photoemission experiment can be seen as an excitation process consisting of the emission of a core electron, followed by the relaxation of the valence electrons in order to screen the resulting localized positive charge. Measured binding energy corresponds thus to the total-energy difference between the fully relaxed system and the unperturbed one. In the so-called initial-state approximation,[32] the value of a core-level shift between clean and adsorbate-covered surface is approximated by the difference in the respective core eigenvalue energies between the two systems. Since the degree of screening on a clean and adsorbate covered surface may be different, this approximation neglects the ''final-state'' effects. However, existing results on the relative importance of the initial- and final- state contributions show that in most materials, the overall evolution of the core electron binding energies is principally controlled by the initial-state effects. In the following we will thus consider only the initial-state contribution.

Results on the calculated shift of surface Ag $3d$ and Ge $3d$ core levels are summarized in Figs. 6(a) and 6(b), respectively. In the case of Ag $3d$ core levels, our results show that in all cases the adsorbate-induced shift compensates the surface core-level shift and even goes beyond, the modification being very sensitive to both adsorption site and Ge coverage. On the one hand, for the lowest coverage considered (0.25 ML or isolated atoms) we find an increase of the binding

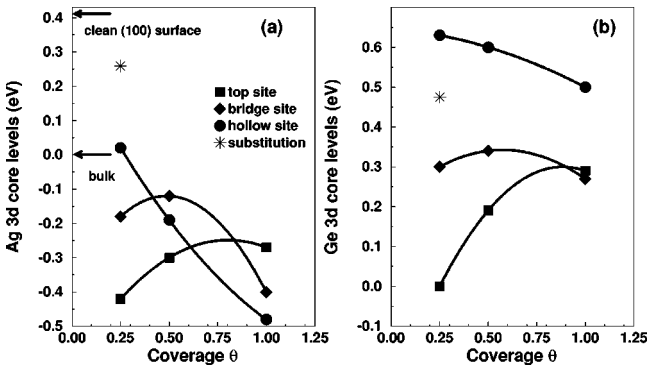

FIG. 6. Calculated shifts of Ag 3*d* (a) and Ge 3*d* (b) core states as a function of the adsorption site and Ge coverage. For Ag 3*d* the energy of the bulk core level is taken as a reference. The shift of Ge 3*d* states is given with respect to the on-top adsorption of an isolated Ge adatom.

energy from the hollow to the on-top site. Since for this coverage, regardless the adsorption geometry, surface Ag atom has a single Ge first neighbor, this evolution reflects the increase of the Ge-Ag bond strength when passing from the more to the less coordinated adsorption sites. It is worth noticing, that single Ge-Ag bond (hollow site) is enough to compensate the surface core levels shift, which means that one has to be carefull when trying to define a metallic character for adsorption, the Ge-Ag bond being definitely stronger than any metallic bond of Ag-Ag type. On the other hand, for adsorption in the hollow site, the binding energy increases monotonously (i.e., core levels shift towards lower energies) with the Ge coverage. This is principally due to the increasing number of Ag-Ge bonds and thus to higher coordination of surface Ag atoms. Similarly, for 1.0 ML coverage, when passing from on-top to bridge and to hollow adsorption site, the number of first Ge neighbors increases and so does the binding energy. However this simple systematics, showing the influence of both Ag-Ge bond strength and number of Ge neighbors, does not hold throughout all the considered cases. Indeed at the early growth stage, as a function of the Ge coverage, the binding energy clearly increases for Ge adsorbed in the surface hollow site, whereas otherwise it decreases. This information can directly serve to determine the preferential adsorption site of isolated Ge atoms from experimental results taken at very low Ge coverage. Additionally, since the calculated shift of Ag 3*d* levels induced by a substitutional Ge atom is considerably smaller compared to any surface adsorption case, photoemission experiments can potentially be used also for determination of the adsorption mode. Finally, it is worth underlining that the calculated shifts of the Ag 3*d* states correlate well with the displacements of the Ag 4*d* valence band reported in the preceding sections.

Similarly, the Ge 3*d* core levels are relatively sharp and the technique of low energy diffraction spectroscopy can be successfully used to examine also this level at existing synchrotron radiation sources. In Fig. 6(b), we have represented the Ge 3*d* level shifts with respect to an arbitrary reference: the isolated Ge adatom adsorbed on-top of surface Ag. The main characteristics of the evolution of the binding energy correspond well to what is found for the Ag 3*d* levels. Again, although the same tendency does not hold in the whole coverage range, the initial evolution as a function of coverage is significantly site dependent: binding energy of Ge 3*d* levels increases if Ge adsorbs in the hollow site and decreases otherwise.

B. Simulated STM images

In the last decade STM has become a wide spread tool for surface characterization. The atomic scale resolution which can be achieved by modern microscopes makes also possible to use this technique for studies of surface adsorption and of early stages of surface growth. However, it has been pointed out that since what is registered by the probe corresponds to a superposition of structural and electronic effects, direct extraction of structural characteristics from STM images often requires some caution. In this domain, the covalent systems, for which delocalization of electronic charge along the interatomic bonds is strong, constitute a classical example. Approximations of different level of sophistication have been elaborated in order to model efficiently the interaction of the STM tip with the surface, to calculate the tunneling current and thus to simulate the STM images. Many questions concerning the relative weights of different approximations remain still unanswered. In the following we take into account the electronic effects at the most basic level of approximation, in which the tunneling current is considered as proportional to the surface electron density of electrons in the Fermi level region.

In Fig. 7 we show the contour plots of electron density in the region of ± 0.5 eV around Fermi energy for an isolated Ge adatom on the Ag(100) surface in the three different adsorption geometries. The left and right panels represent the cross-sections in planes perpendicular and parallel to the Ag(100) surface, respectively. For all the three adsorption geometries the horizontal miscut plane was taken at 2.67 Å from the surface.

Focusing on the left panel one clearly sees that the amplitude of the corrugation due to the adsorbed Ge adatom depends substantially on the adsorption site. Using an arbitrary $\rho = 1 \times 10^{-3}$ e/au^3 contour for the three adsorption geometries we find its corrugation to be equal to 2.38 Å, 2.76 Å, and 3.10 Å for the hollow, bridge, and on-top adsorption sites. This evolution reflects principally the difference of local packing of atoms: a Ge adatom integrates itself into the surface the most when adsorbed in a hollow site, and the less when adsorbed on-top of a surface Ag atom. Using the calculated nearest-neighbor bond lengths (Fig. 5), the equilibrium spacings between the Ge adatom and the Ag (100) surface are found to be equal to 1.61 Å, 1.97 Å, and 2.33 Å for the hollow, bridge, and on-top adsorption sites. Thus, although taking into account the spatial distribution of electrons makes the corrugation larger (the same conclusion can be obtained simply from comparison of Ag and Ge atomic radii), the changes of the electronic distribution as a function of adsorption geometry remain small. It is thus likely that use of more sophisticated modeling tools in order to account for electronic contributions would not alter present conclusions. It is also worth noticing that the recent results, obtained by electronic scattering quantum chemistry ESQC method for Ga/Ag(100),[28] give surface corrugations of 2.11 Å, 2.35 Å, and 2.87 Å for the hollow, bridge, and on-top adsorption

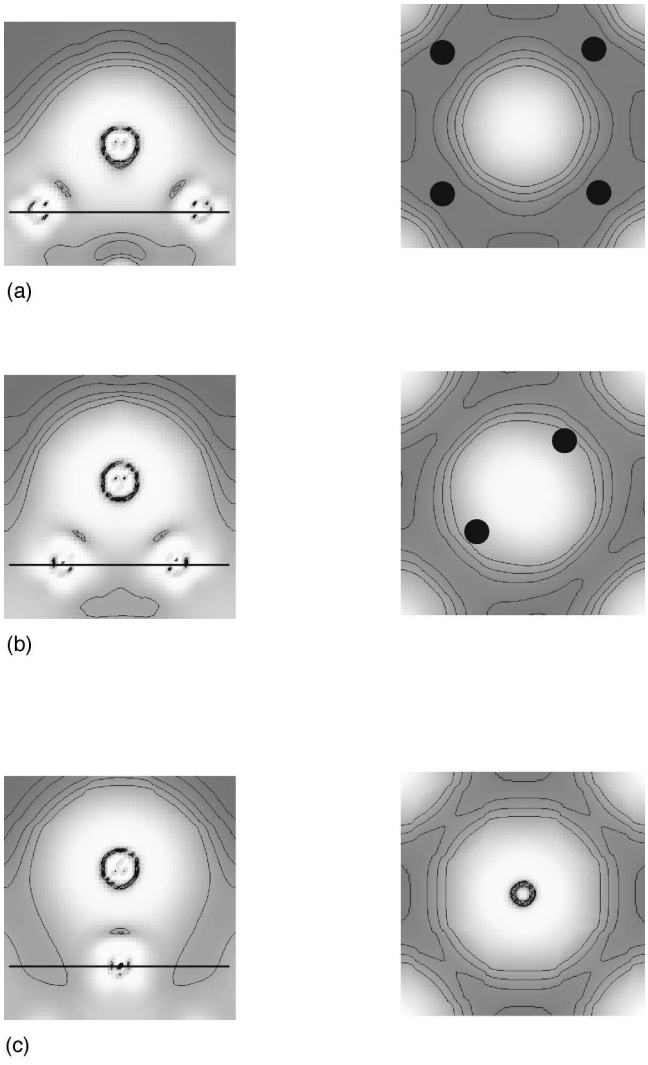

FIG. 7. Electron density at the Fermi level, for the Ge adatom in the hollow (a), on-bridge (b), and on-top (c) adsorption sites. The cross-sections in the planes perpendicular and parallel to the surface (100) are depicted in the left and right columns, respectively. Black dots indicate the positions of surface Ag atoms.

sites, showing not only the same evolution as a function of the adsorption site, but also very similar differences in calculated corrugations between different adsorption geometries.

The influence of the adsorption-induced distortion of the Ge adatoms can be estimated using the horizonal cross sections (right panel). Although in all cases adsorbed atoms remain basically spherical, for adsorption on the bridge site we find a small elliptical distortion of the electron density. The apparent size of the adatom is the largest for adsorption on-top of surface Ag atoms and the smallest for adsorption in the hollow site, reflecting calculated corrugation heights.

V. CONCLUSIONS

Using the *ab initio* FP-LMTO approach we have studied the characteristics of Ge adsorption on the Ag (100) surface. For isolated Ge adatoms we find a strong preference to maximize the number of bonds with the surface and thus to adsorb in the surface hollow sites. The progressive increase of the adsorbate-substrate bond length as a function of increasing number of bonds, reflects a well-known many-body character of interactions proposed already for purely metallic systems. From this point of view, Ge should then present a quasi-metallic behavior with respect to adsorption. For higher coverage, results obtained for model epitaxial Ge deposits show that although the energetical preference of Ge to adsorb in the hollow site is still present, increasing coverage reduces the differences between the three adsorption geometries. This suggests that the direct Ge-Ge interaction can become competitive with the adsorption energetics and that as a consequence a Ge deposit can reconstruct, recovering partially its covalent character. By analyzing the adsorption-induced modifications of the electronic structure of the substrate and of the adsorbate as a function of adsorption geometry and coverage, we were able to extract some very clear tendencies. The drastic deformation of Ag LDOS due to Ge bonds clearly puts some limits to a pure metallic-like character of Ge/Ag adsorption. Moreover, especially for low coverage rates, they can be used for the interpretation of experimental results. In particular we have analyzed the evolution of the substrate valence band and both substrate and adsorbate core level binding energies. Coupled to experimental results, these findings should allow to describe the changes in the atomic structure of the Ge deposit as a function of the coverage. Finally by a simple approach we have simulated the STM images of Ge adatoms on the Ag(100) surface. Our results show that differences in surface corrugation for different adsorption geometries are related principally to the positions of atoms, the electronic contribution being practically negligible. On the other hand, strong dependence of the calculated corrugation on the adsorption geometry can reveal useful for practical determination of atomic positions from STM images of complex reconstructed structures.

ACKNOWLEDGMENTS

We thank A. Saúl, H. Oughadou, B. Aufray, J. M. Gay, and G. Lelay for helpful discussions during the course of this work. The most time-consuming calculations were performed on the CRAY C98 computer at IDRIS, under Project No. 980732. We are grateful for a generous allocation of time on the machine. The CRMC[2] is also associated with the Universities of Aix-Marseille II and III.

[1] S. M. Sze, *Physics of Semiconductor Devices*, 2nd ed. (Wiley, New York, 1981).

[2] M. Göthelid, M. Hammar, U.O. Karlsson, C. Wigren, and G. LeLay, Phys. Rev. B **52**, 14 104 (1995).

[3] A. Samsavar, T. Miller, and T.-C. Chiang, Phys. Rev. B **38**, 9889 (1988).

[4] M. del Giudice, J.J. Joyce, M.W. Ruckman, and J.H. Weaver, Phys. Rev. B **32**, 5149 (1985).

[5] A.L. Wachs, T. Miller, and T.-C. Chiang, Phys. Rev. B **33**, 8870 (1986).
[6] G. Brocks, P.J. Kelly, and R. Car, Phys. Rev. Lett. **70**, 2786 (1993).
[7] H.H. Weitering and J.M. Carpinelli, Surf. Sci. **384**, 240 (1997).
[8] D.J. Spence and S.P. Tear, Surf. Sci. **398**, 91 (1998).
[9] M.W. Ruckman, M. del Giudice, and J.H. Weaver, Phys. Rev. B **32**, 1077 (1985).
[10] M.W. Ruckman, M. del Giudice, J.J. Joyce, and J.H. Weaver, Phys. Rev. B **33**, 8039 (1986).
[11] C. Polop, J.L. Sacedón and J.A. Martín-Gagon, Surf. Sci. **402**, 245 (1998).
[12] H. Oughaddov, J. M. Gay, B. Aufray, L. Lapenaz, G. Lelay, O. Bunk, J. H. Zeysing, and R. L. Johnson (unpublished).
[13] P. Hohenberg and W. Kohn, Phys. Rev. **136**, B864 (1964).
[14] W. Kohn and L.J. Sham, Phys. Rev. **140**, A1133 (1965).
[15] D.M. Ceperley and B.J. Alder, Phys. Rev. Lett. **45**, 566 (1980).
[16] M. Methfessel, Phys. Rev. B **38**, 1537 (1988).
[17] M. Methfessel, C.O. Rodriguez, and O.K. Andersen, Phys. Rev. B **40**, 2009 (1989).
[18] M. Methfessel, D. Hennig, and M. Scheffler, Phys. Rev. B **46**, 4816 (1992).
[19] J.N. Andersen, D. Hennig, E. Lundgren, M. Methfessel, R. Nyholm, and M. Scheffler, Phys. Rev. B **50**, 17 525 (1994).
[20] C. Kittel, *Introduction to Solid State Physics* (Wiley, New York, 1986); L. Pauling, J. Am. Chem. Soc. **53**, 1367 (1931).
[21] P. Hermann, D. Simon, and B. Bigot, Surf. Sci. **350**, 301 (1996).
[22] J.-F. Paul and P. Sautet, Phys. Rev. B **53**, 8015 (1996).
[23] D. Jentz, S. Rizzi, A. Barbieri, D. Kelly, M.A. Van Hove, and G.A. Somorjai, Surf. Sci. **329**, 14 (1995).
[24] W. Eberhardt, S.G. Louie, and E.W. Plummer, Phys. Rev. B **28**, 465 (1983).
[25] M.C. Desjonquères and D. Spanjaard, *Concepts in Surface Physics*, 2nd ed. (Springer, Berlin, 1995).
[26] B.D. Yu and M. Scheffler, Phys. Rev. B **56**, 15 569 (1997).
[27] H. Huang, H. Over, S.Y. Tong, J. Quinn, and F. Jona, Phys. Rev. B **49**, 13 483 (1994).
[28] D.E. Bürgler, P. Hermann, S. Corbel, C.M. Schmidt, D.M. Schaller, P. Sautet, A. Baratoff, and H.-J. Güntherodt, Phys. Rev. B **57**, 10 035 (1998).
[29] R. Dudde, H. Bernhoff, and B. Reihl, Phys. Rev. B **41**, 12 029 (1990).
[30] J.H. Weaver, A. Franciosi, and V.L. Moruzzi, Phys. Rev. B **29**, 3293 (1984).
[31] A. Franciosi, D.W. Niles, G. Margaritondo, C. Quaresima, M. Capozi, and P. Perfetti, Phys. Rev. B **32**, 6917 (1985).
[32] D. Spanjaard, C. Guillot, M.C. Desjonquères, G. Tréglia, and J. Lecante, Surf. Sci. Rep. **5**, 1 (1985).